Scientific Journal of the Ternopil National Technical University
2026, vol. 121, no. 1, pp. 4–19,
ISSN: 2522-4433 Print, ISSN: 2522-4441 Online
https://doi.org/10.33108/visnyk_tntu2026.01.004

Submitted: 2025-11-08 | Revised: 2026-02-01 | Accepted: 2026-03-24

From ceramic core to metal rich surface: functionally graded Al_2O_3-Ni composites fabricated by centrifugal gel casting

Justyna Zygmuntowicz[1*], Joanna Tańska[2], Paulina Wiecińska[2], Paulina Piotrkiewicz[1], Katarzyna Konopka[1], Mikołaj Szafran[2], Marcin Wachowski[3], Joanna Szymańska[4], Waldemar Kaszuwara[1]

[1] Warsaw University of Technology, Faculty of Materials Science and Engineering, 141 Woloska St., 02-507 Warsaw, Poland

[2] Faculty of Chemistry, Warsaw University of Technology, 3 Noakowskiego St., 00-664 Warsaw, Poland

[3] Military University of Technology, Faculty of Mechanical Engineering, gen. S. Kaliskiego 2 St., 00-908 Warsaw, Poland

[4]Imerys Technology Center, 1 rue Le Chatelier, 38090 Vaulx-Milieu, France

***** Corresponding author Justyna.zygmuntowicz@pw.edu.pl

Abstract: *Functionally graded Al_2O_3-Ni composites were fabricated by centrifugal gel casting using a suspension with a total solid loading of 55 vol.% and a metallic phase content of 10 vol.% Ni. The applied centrifugal field induced a pronounced radial redistribution of the metallic phase, resulting in a three-zone microstructure consisting of a Ni-rich outer region, a transition zone, and a ceramic-dominated inner region. Archimedes' measurements revealed a high relative density of 99.24 ± 0.74%, low open porosity of 3.54 ± 0.52%, and minimal water absorption of 0.79 ± 0.10%, confirming effective densification. Linear shrinkage after sintering at 1400°C in an Ar/H_2 atmosphere was 13.67% in the axial direction and 13.30% in the radial direction, corresponding to a volumetric shrinkage of 35.24%. Quantitative image analysis showed a local nickel volume fraction of up to 23% in the outer zone and approximately 1% in the inner zone. The mean equivalent diameter of Ni particles ranged from 1.77 to 2.08 μm, depending on the radial position. The alumina matrix exhibited a fine-grained microstructure with a mean grain size of 0.43 ± 0.21 μm. EDS analyses confirmed a smooth compositional gradient and chemical stability of the Al_2O_3-Ni interfaces without secondary phase formation. These results demonstrate that centrifugal gel casting is an effective method for producing dense, chemically stable, and functionally graded ceramic-metal composites with a controlled microstructural architecture.*

Keywords: *Centrifugal gel casting, Functionally graded materials, Al2O3-Ni composites, Microstructural gradient, Ceramic-metal composites.*

1. INTRODUCTION

Ceramic-metal composites and ceramic-based functionally graded materials (FGMs) have attracted sustained interest due to their ability to combine the hardness, stiffness, and thermal stability of ceramics with the toughness, electrical conductivity, and damage tolerance of metals [1–4]. These materials are ideal for applications requiring spatially tailored properties, such as wear-resistant components, thermal barriers, electronic substrates, and energy-related systems [5–8]. However, achieving a controlled distribution of metallic phases within a ceramic matrix remains a significant challenge. Conventional powder processing routes often result in agglomeration, poor interfacial bonding, or uncontrolled phase segregation [10–12].

Wet-process molding techniques are widely used to fabricate ceramic-metal composites because they allow for homogeneous powder dispersion, high solid loading, and near-net-shape forming [13–15]. Common approaches include slip casting, tape casting, gel casting, and colloidal filtration [16–21]. Among these techniques, gel casting has gained particular attention due to its ability to immobilize complex green bodies through in situ polymerization, resulting in high green strength and low defect density. Properly designed gel casting enables precise control of rheological behavior and particle packing, which is crucial for producing dense, crack-free ceramic-metal composites after sintering [20].

Centrifugal forming techniques are a powerful extension of conventional wet processing routes because they introduce an external force field that actively redistributes phases according to their density, size, and shape [22]. In centrifugal slip or gel casting, the combined action of centrifugal acceleration and controlled gelation allows for the production of functionally graded structures in a single processing step [22]. For ceramic-metal systems with significant density differences, such as Al_2O_3-Ni, centrifugal forces can induce a gradual compositional gradient, eliminating the need for layer-by-layer deposition or multiple casting cycles. Compared to traditional fabrication methods for functionally graded materials (FGM), such as powder stacking, hot pressing of layered compacts, or additive manufacturing, centrifugal gel casting offers advantages in simplicity, scalability, and microstructural continuity.

Despite its advantages, centrifugal gel casting for ceramic-metal composites remains relatively unexplored, particularly in terms of the quantitative relationships between processing conditions, phase redistribution, densification behavior, and microstructural refinement. Challenges persist in maintaining slurry stability during centrifugal processing, controlling gelation kinetics to prevent excessive phase segregation, and ensuring chemical compatibility between the ceramic and metallic phases during high-temperature sintering. Additionally, detailed microstructural analyses resolving local variations in particle size, volume fraction, and chemical composition across graded regions are limited in the literature.

In this context, the present study investigates the fabrication of functionally graded Al_2O_3-Ni composites using centrifugal gel casting combined with pressureless sintering in a reducing atmosphere. This work systematically examines densification behavior, shrinkage characteristics, and microstructural evolution across the radial direction of the composites. Particular emphasis is placed on the quantitative analysis of nickel phase distribution, particle size variation, and alumina grain refinement in the distinct microstructural zones formed during centrifugal processing. Advanced scanning electron microscopy (SEM)-based image analysis and energy dispersive spectroscopy (EDS) measurements are employed to provide direct chemical and morphological evidence of phase stability and gradient continuity.

This research is novel because it demonstrates that centrifugal gel casting can form dense, chemically stable Al_2O_3-Ni composites with a well-defined, three-zone, radial architecture while maintaining near-isotropic shrinkage and submicrometer ceramic grain size. Coupling controlled gelation with centrifugal phase segregation provides new insights into the mechanisms governing microstructural grading in ceramic-metal systems. This work establishes centrifugal gel casting as a viable, versatile method for designing functionally graded composites with tailored property distributions. These results expand our understanding of wet-processing strategies for advanced ceramic-metal materials, opening new opportunities for their use in components that require spatially optimized performance.

It should be emphasized that functionally graded materials (FGMs) are designed so that their composition and properties vary gradually within a single component [23–26]. Such materials are highly attractive for applications where different regions must simultaneously resist wear, carry load, conduct heat or electricity, or tolerate thermal and mechanical gradients. However, controlling these gradients during manufacturing remains one of the key challenges

in materials science. In this work, a distinctly different and more controllable approach to fabricating ceramic-metal FGMs was demonstrated by combining centrifugal casting with in situ gelation. This method overcomes key limitations of existing fabrication routes and enables the production of dense, chemically stable Al_2O_3-Ni composites with a smooth, continuous microstructural gradient.

In conventional centrifugal slip casting, phase segregation is driven solely by centrifugal forces acting on a fluid suspension [27–28]. While this can induce some degree of grading, the process suffers from several inherent drawbacks, including uncontrolled sedimentation, blurring of gradients, and defect formation. Metallic particles continue to migrate as long as the suspension remains fluid, often leading to excessive segregation or particle agglomeration [27]. Without a rapid immobilization mechanism, the final microstructure can be sensitive to minor variations in processing time and viscosity. Prolonged particle motion increases the risk of density gradients, pore accumulation, and microcracking during drying and sintering [27]. As a result, conventional centrifugal slip casting often produces poorly defined or irreproducible gradients, especially in ceramic-metal systems with large density contrasts.

The present work introduces in situ gelation during centrifugal processing, fundamentally changing how the microstructure develops. Phase redistribution occurs first, driven by centrifugal forces. Gelation then rapidly increases viscosity, effectively «freezing» the particle distribution in place. The resulting microstructure is stable, reproducible, and well-defined, forming a three-zone architecture: a metal-rich outer region, a transition zone, and a ceramic-dominated inner core. This coupling of centrifugal segregation with controlled gelation enables precise microstructural control that cannot be achieved by centrifugal slip casting alone.

Layer-by-layer fabrication methods, including tape stacking, powder layering, and many additive manufacturing techniques, are widely used to create FGMs [29–31]. However, they also introduce their own challenges, such as discrete interfaces, Interfacial stresses, processing complexity, or material constraints. Even when layers are thin, compositional changes often occur in a stepwise manner rather than continuously. Sharp transitions between layers can act as stress concentrators, increasing the risk of delamination or cracking [29–31].

Multi-step deposition, alignment, and bonding significantly increase fabrication time and cost. Many ceramic–metal systems are difficult to process via additive manufacturing due to powder reactivity, oxidation, or thermal mismatch.

In contrast, the centrifugal gel casting approach demonstrated in this work produces a continuous compositional gradient in a single forming step. Eliminates discrete interfaces between layers. Avoids complex toolpaths, layer registration, or post-bonding treatments. It is compatible with high solid loading and pressureless sintering, enabling near-theoretical densification. Rather than «building» a gradient layer by layer, this method lets the gradient self-form under physical forces, then stabilizes it through gelation. This research goes beyond demonstrating a new processing route. It provides quantitative insight into how graded microstructures form and stabilize. The study shows how nickel particle size and volume fraction vary systematically with radial position, revealing the interplay between centrifugal forces. Despite strong compositional gradients, the composites exhibit near-isotropic shrinkage and high densification, addressing a long-standing concern in FGM processing. Chemical analysis confirms that the Al_2O_3-Ni system remains chemically stable during sintering, with no formation of deleterious reaction phases. These findings advance the fundamental understanding of microstructure evolution in ceramic-metal FGMs. The approach opens new opportunities for advanced structural and functional components in applications where continuous property gradients are essential.

2. METHODS

2.1. Starting materials

Commercial alumina (Al_2O_3) powder was used as the ceramic matrix material, while nickel (Ni) powder served as the metallic reinforcing phase. The total solid loading of the casting suspension was fixed at 55 vol.%, with the metallic phase constituting 10 vol.% of the total solid content. The selected powder system was chosen to enable the fabrication of ceramic–metal composites with a pronounced density contrast between phases, facilitating controlled phase redistribution during centrifugal processing.

2.2. Preparation of suspension

The ceramic-metal suspension was prepared by dispersing the Al_2O_3 and Ni powders in a liquid medium containing appropriate dispersing and gelling agents. The powders were added gradually under continuous stirring to ensure homogeneous distribution and to prevent agglomeration. The slurry composition and solid loading were optimized to obtain sufficient fluidity for centrifugal casting while maintaining high green density after gelation. Prior to casting, the suspension was degassed to remove entrapped air bubbles that could lead to defects in the green bodies.

2.3. Centrifugal gel casting process

Centrifugal gel casting was employed to fabricate functionally graded Al_2O_3-Ni composites. The prepared suspension was poured into cylindrical molds and subjected to centrifugal rotation, inducing a radial acceleration field. Due to the higher density of nickel compared to alumina, the metallic particles migrated preferentially toward the outer region of the mold during rotation. Gelation was initiated during centrifugal processing, progressively increasing the viscosity of the suspension and immobilizing the spatial distribution of the solid phases. This combination of centrifugal forces and in situ gelation enabled the formation of a stable, radially graded microstructure without macroscopic phase separation or sedimentation defects. After completion of the gelation process, the green bodies were demoulded and dried under controlled conditions to minimize cracking and distortion.

2.4. SINTERING PROCEDURE

The dried green samples were sintered in a reducing Ar/H_2 atmosphere to prevent oxidation of the nickel phase and to maintain chemical stability at the Al_2O_3-Ni interfaces. The thermal cycle consisted of heating at a rate of 1°C/min up to 600°C to ensure uniform removal of organic components, followed by heating at 2°C/min up to 1400°C. The samples were held at the maximum temperature for 2 hours to promote densification, and then cooled at a rate of 2°C/min to room temperature. This sintering schedule was designed to achieve high densification while limiting excessive grain growth of the alumina matrix.

2.5. PHYSICAL PROPERTY MEASUREMENTS

The relative density, open porosity, and water absorption of the sintered composites were determined using the Archimedes method. Measurements were performed in accordance with standard procedures, and the results were calculated as averages from multiple specimens to ensure reproducibility.

Linear shrinkage was determined by measuring the sample dimensions before and after sintering along both the axial direction (sample height) and the radial direction (outer diameter). Volumetric shrinkage was calculated based on the measured linear shrinkage values.

2.6. MICROSTRUCTURAL CHARACTERIZATION

The microstructure of the sintered composites was examined using scanning electron microscopy (SEM) operated in backscattered electron (BSE) mode to enhance compositional contrast between the alumina matrix and the nickel phase. Polished cross-sections perpendicular to the rotation axis were prepared for analysis. Quantitative image analysis was performed to determine the local volume fraction and size distribution of nickel particles in different radial regions of the samples.

Energy-dispersive X-ray spectroscopy (EDS) was employed for both line-scan and point analyses to assess the radial distribution of elements and verify the chemical stability of the Al_2O_3-Ni interfaces. Grain size analysis of the alumina matrix was performed by measuring the equivalent grain diameter (d_2) from SEM images, and the results were presented as histograms to assess the grain size distribution after sintering.

3. RESULTS

The article evaluated the physical properties of the Al_2O_3-Ni composites fabricated by centrifugal gel casting using the Archimedes method to determine their relative density, open porosity, and water absorption. The composites' measured relative density reached $99.24 \pm 0.74\%$ of the theoretical density. This indicates a high degree of densification, confirming the effectiveness of the forming and sintering procedures. The open porosity of the samples was found to be $3.54 \pm 0.52\%$, consistent with the high relative density values, suggesting that most residual pores are closed or isolated. This limited porosity suggests efficient packing of the solid phase in the green body and controlled pore elimination during sintering, despite the presence of a metallic phase and a functionally graded microstructure induced by centrifugal processing. Consequently, the water absorption was low at $0.79 \pm 0.10\%$, further confirming the compact nature of the microstructure and the restricted connectivity of the open pores. This low water uptake is significant for potential structural and functional applications because it reflects good resistance to fluid penetration and environmental degradation. Archimedes' measurements demonstrate that centrifugal gel casting produces Al_2O_3-Ni composites with near-theoretical density, low open porosity, and minimal water absorption. These results validate the effectiveness of the processing method for producing dense ceramic-metal composites with stable physical properties, providing a solid foundation for understanding the observed mechanical and microstructural performance.

In the next step, an experiment was conducted to estimate the shrinkage behavior of the Al_2O_3-Ni composite fabricated using the centrifugal gel casting method by measuring both linear and volumetric dimensional changes after sintering. Linear shrinkage, as determined by measuring the sample height, was 13.67%. Linear shrinkage, as measured along the outer diameter of the cylindrical specimen, was slightly lower at 13.30%. This close agreement indicates a high degree of dimensional uniformity, suggesting that shrinkage during sintering was nearly isotropic, despite the functionally graded microstructure induced by centrifugal processing. The composite's total volumetric shrinkage was calculated to be 35.24%, consistent with the measured linear shrinkage values and typical of alumina-based composites with high solid loadings formed by gel casting. This level of volumetric contraction reflects effective particle packing in the green

body and efficient densification during sintering, while avoiding excessive differential shrinkage that could lead to cracking or distortion. The marginal difference between axial and radial shrinkage can be attributed to the radial compositional gradient inherent to the centrifugal gel casting process. However, the limited magnitude of this difference shows that redistribution of the nickel phase does not significantly disrupt overall sintering uniformity. These results confirm that the selected slurry composition, gelation conditions, and sintering schedule provide adequate control over dimensional stability. The obtained shrinkage values suggest that centrifugal gel casting can be used to fabricate Al_2O_3-Ni composites with predictable and reproducible densification behavior. This is important for producing near-net-shape components and maintaining dimensional tolerances in advanced structural and functional applications. The formation of radially graded Al_2O_3-Ni composites by centrifugal gel casting inherently introduces spatial variations in metallic phase content and local packing density. In principle, such heterogeneities could promote anisotropic shrinkage during sintering due to differential densification rates across the sample cross-section. However, the present results demonstrate that shrinkage anisotropy remains minimal, as evidenced by the close agreement between axial and radial linear shrinkage values. This behavior can be rationalized by considering the combined effects of green body homogeneity, sintering mechanisms, phase distribution continuity, and mechanical constraint during densification. Although the nickel phase exhibits a pronounced radial gradient, the alumina matrix forms a continuous, load-bearing skeleton throughout the entire volume of the composite. The gel casting process ensures homogeneous dispersion of the ceramic particles at the green state and suppresses sedimentation-induced defects prior to gelation. As a result, variations in local packing density are primarily associated with the redistribution of the metallic phase rather than with large-scale heterogeneities in the ceramic framework. Since sintering shrinkage in ceramic–metal composites is governed predominantly by the densification of the ceramic matrix, the relatively uniform green density of the Al_2O_3 network leads to comparable densification kinetics in both radial and axial directions. The nickel particles act as inclusions embedded within this continuous ceramic skeleton and do not disrupt the global continuity of the sintering path. A key factor limiting shrinkage anisotropy was the absence of abrupt compositional interfaces in these composites. The centrifugal gel casting process produces a smooth, continuous transition in nickel content from the outer to the inner region, rather than discrete layers with sharply differing compositions. This graded architecture distributes local strain incompatibilities over a finite radial distance, reducing the driving force for differential shrinkage and stress accumulation. From a sintering mechanics perspective, sharp interfaces between regions with different densification rates are more prone to constrained shrinkage and anisotropic deformation. In contrast, the gradual gradient observed here allows local densification strains to be accommodated elastically and plastically by neighbouring regions, thereby maintaining overall dimensional uniformity. The in situ gelation step should also be considered, as it plays a crucial role in stabilizing the green body structure. Once gelation occurs, particle rearrangement is effectively suppressed, and the spatial distribution of both ceramic and metallic phases is fixed. This early immobilization prevents post-casting sedimentation or rearrangement that could otherwise lead to large density gradients or preferred densification paths. As a result, the green body entering the sintering stage already exhibits a mechanically coherent structure with isotropic connectivity. This structural coherence translates into uniform macroscopic shrinkage, despite variations in microscopic phase fractions that occur radially. Although nickel is distributed heterogeneously, its influence on the sintering kinetics of alumina is limited under the applied conditions. The sintering was conducted at 1400°C in a reducing Ar/H_2 atmosphere, where alumina undergoes solid-state sintering

without the formation of a liquid phase. The nickel phase remains metallic and chemically stable, as confirmed by EDS analysis (discussed later in the manuscript), and does not actively participate in mass transport processes governing ceramic densification.

Consequently, local variations in nickel content do not translate into substantial differences in the densification rate of the alumina matrix. Instead, nickel particles primarily act as inert inclusions that may locally constrain grain boundary motion but do not impose a dominant directional constraint on macroscopic shrinkage. The observation of low shrinkage anisotropy in the presence of strong radial gradients demonstrates that centrifugal gel casting enables the fabrication of functionally graded ceramic–metal composites without sacrificing dimensional stability. This finding is particularly significant for near-net-shape manufacturing, where anisotropic shrinkage can lead to distortion, cracking, or loss of dimensional tolerance.

By ensuring a continuous ceramic skeleton, controlled gelation, and smooth compositional gradients, the process decouples microstructural grading from macroscopic deformation. This provides a robust framework for designing FGMs with tailored spatial properties while maintaining predictable and reproducible sintering behavior.

The microstructure of the Al_2O_3-Ni composite, which was fabricated using centrifugal gel casting with a total solid content of 55 vol.% and a metallic phase content of 10 vol.% Ni, exhibits pronounced radial heterogeneity. This heterogeneity results from the combined action of centrifugal forces and density differences in phase during formation. Backscattered electron scanning electron microscopy (BSE-SEM) observations reveal the formation of a distinct three-zone structure (Zones I-III) across the sample cross-section, as indicated schematically in Figure 1. Zone I (the outer region near the mold wall) is characterized by a high concentration of visible nickel particles as uniformly distributed bright contrast regions within the alumina matrix. In this zone, the Ni phase forms a dense, quasi-continuous network composed predominantly of fine, equiaxed particles with limited interparticle spacing. This microstructural arrangement is attributed to the higher density of nickel relative to alumina, which promotes the preferential migration of the metallic phase toward the outer radius under centrifugal acceleration. Zone I's alumina matrix appears relatively compact, with low residual porosity, indicating effective particle packing and efficient removal of excess liquid during the casting process. The proximity of the Ni particles to the ceramic matrix indicates favourable mechanical interlocking and the potential for improved load transfer.

Zone II (the transition region) shows a gradual decrease in nickel content, accompanied by a noticeable change in particle morphology and spatial distribution. In this intermediate zone, the Ni particles are less densely packed, showing increased elongation and partial alignment in the radial direction. The metallic phase is discontinuously distributed, forming clusters and chains embedded within the alumina matrix. Zone II represents a compositional and microstructural gradient rather than a sharp interface, indicating the progressive redistribution of the metallic phase during centrifugal gelation. The alumina matrix remains continuous; however, local variations in contrast suggest slight differences in packing density and residual porosity compared to Zone I. Such a graded microstructure is characteristic of centrifugal forming methods and advantageous for reducing stress concentrations between regions of differing composition.

Zone III, the inner region near the rotation axis, is dominated by an alumina ceramic matrix with a sparse, finely dispersed nickel phase. The nickel particles in this zone are small, isolated, and uniformly distributed without evidence of agglomeration. This reduced metallic phase content reflects the limited ability of nickel particles to migrate toward the inner radius against the centrifugal field. Zone III's alumina matrix appears homogeneous and dense with minimal observable microstructural defects at the applied magnification. Therefore, this region

can be considered ceramic-rich and is expected to exhibit properties similar to monolithic alumina. The centrifugal gel casting process successfully produces a functionally graded Al_2O_3-Ni composite with a continuous transition from a metal-rich outer zone to a ceramic-dominated inner zone. The absence of macroscopic defects, sharp interfaces, or large-scale nickel agglomerates indicates good slurry stability and effective control of gelation kinetics during the forming process. The observed microstructural gradient is expected to significantly influence the composite's mechanical response, particularly under compressive and flexural loading, by combining the toughness-enhancing role of the metallic phase with the stiffness and hardness of the ceramic matrix.

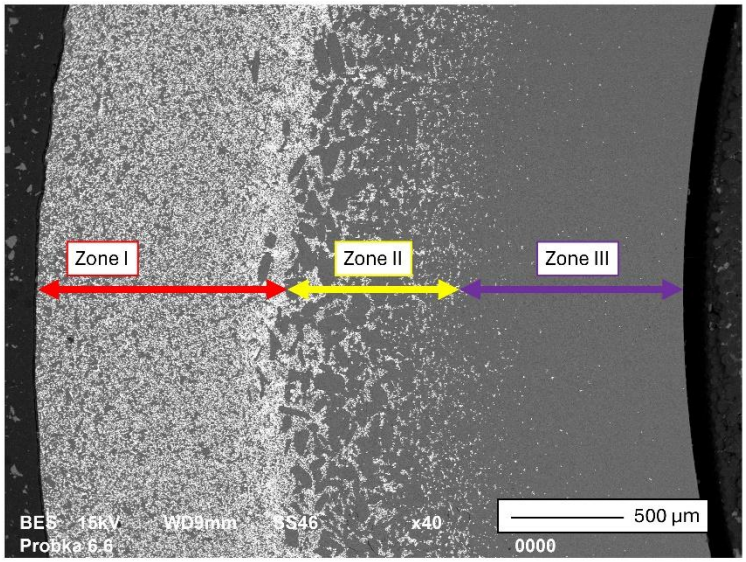

Figure 1. Example of BSE-SEM photographs of a distinct three-zone structure (Zones I–III) across the sample cross-section of Al_2O_3-Ni composites.

Figure 2 presents additional representative BSE-SEM micrographs of the Al_2O_3-Ni composite, along with corresponding histograms that illustrate the size distribution and local volume fraction of the metallic phase in each zone. Zone I (the outer region) has the highest concentration of the metallic phase, with a local nickel volume fraction of $V_v = 23\%$, which is more than twice the nominal amount introduced into the casting suspension. The BSE image confirms the dense dispersion of bright nickel particles that are uniformly embedded in the alumina matrix with limited interparticle spacing. The corresponding histogram shows a dominant population of fine particles with an equivalent diameter of $d_2 = 1.90 \pm 1.79$ µm and a strongly right-skewed distribution. The high frequency of particles below approximately 2 µm suggests that fine nickel particles are effectively transported toward the outer radius under centrifugal acceleration; larger particles appear less frequently. This microstructure indicates efficient phase separation driven by density differences between Ni and Al_2O_3, stabilized by rapid gelation.

Zone II (the transition region) is an intermediate stage of phase redistribution. It has a metallic phase volume fraction of $V_v = 21\%$, which is slightly lower than that observed in Zone I. However, unlike the outer region, Zone II has a more heterogeneous microstructure. A BSE image reveals nickel particles that are clustered locally and regions with reduced metallic content. This reflects incomplete segregation and the dynamic competition between centrifugal forces and increasing slurry viscosity during the gelation process. The particle size histogram shows a broader distribution with a mean equivalent diameter of $d_2 = 2.08 \pm 2.44$ µm, which is the highest among all zones. The increased standard deviation indicates the presence of fine particles as well as a noticeable fraction of coarser nickel agglomerates. These agglomerates are preferentially trapped in the transition zone as the suspension's mobility decreases.

Zone III (the inner region near the rotation axis) is strongly depleted of the metallic phase, with a measured volume fraction of V_v = 1%, which confirms the nearly complete migration of nickel particles toward the outer regions of the sample. The microstructure is dominated by a homogeneous alumina matrix containing only a few, finely dispersed nickel particles. Zone III's histogram shows a narrow particle size distribution with a mean equivalent diameter of d_2 = 1.77 ± 1.14 μm, indicating that the smallest nickel particles primarily remain suspended in this region.

In contrast, larger particles are effectively transported outward during centrifugal casting. Combined microstructural observations and quantitative histogram analysis clearly demonstrate that centrifugal gel casting enables the formation of a functionally graded Al_2O_3-Ni composite. A strong radial gradient in metallic phase content and particle size distribution characterizes this composite. The enrichment of fine nickel particles in Zone I and their progressive depletion toward Zone III confirm the decisive role of centrifugal forces in controlling phase distribution. Conversely, the broadening of the particle size distribution in Zone II underscores the transient nature of the gelation and segregation processes. This graded architecture is expected to significantly impact local mechanical behavior by promoting enhanced toughness and damage tolerance in metal-rich regions while maintaining high stiffness and hardness in ceramic-dominated zones.

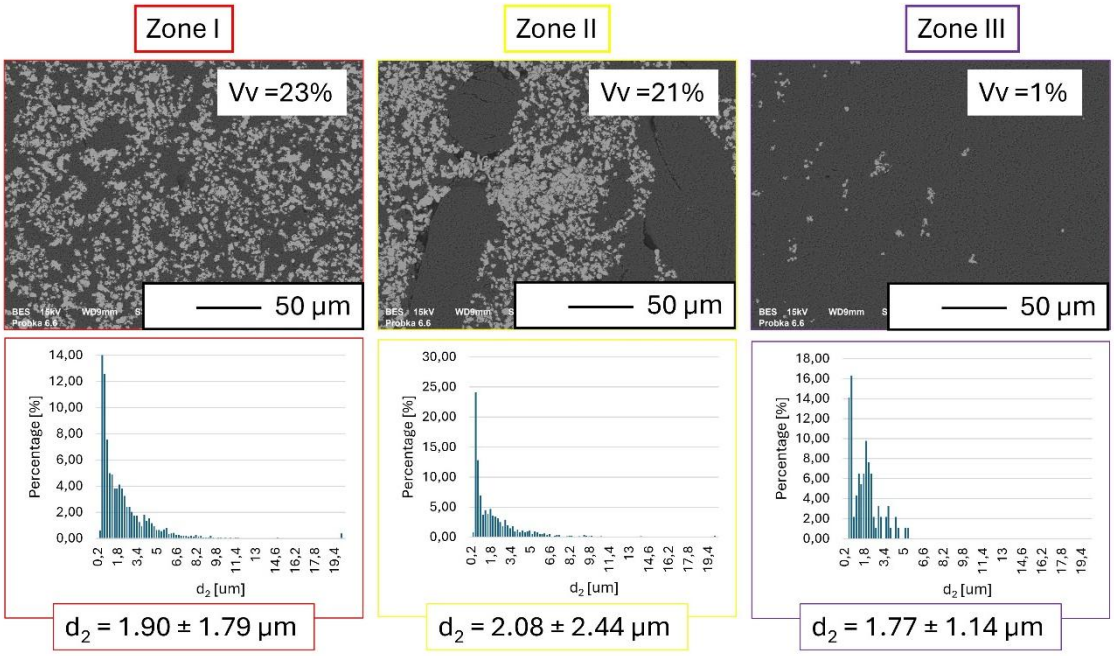

Figure 2. BSE-SEM micrographs of the Al2O3-Ni composite, along with corresponding histograms that illustrate the size distribution and local volume fraction of the metallic phase in each zone.

Figure 3 shows the histogram of the equivalent grain diameter (d_2) of the Al_2O_3 grains in the Al_2O_3-Ni composite after sintering in a reducing Ar/H_2 atmosphere. The thermal schedule consisted of heating at a rate of 1°C per minute up to 600°C, followed by heating at a rate of 2°C per minute up to 1400°C with a two-hour dwell, and then cooling at a rate of 2°C per minute. This sintering profile was selected to promote gradual densification while limiting excessive grain growth of the ceramic matrix. The histogram reveals a unimodal, right-skewed grain size distribution characteristic of fine-grained alumina subjected to controlled solid-state sintering. The mean d_2 is 0.43 ± 0.21 μm, indicating that submicrometer grains dominate the microstructure. The highest frequency of Al_2O_3-Ni grains is observed in the size range of approximately 0.25–0.45 μm,

accounting for the majority of the measured population. This narrow peak indicates the effective suppression of abnormal grain growth during high-temperature exposure. A gradual decrease in frequency is observed for grain sizes exceeding approximately 0.6 μm, forming a pronounced tail that extends up to around 1.2 μm. The low fraction of coarser grains suggests that grain coarsening was spatially limited, preventing the formation of a bimodal distribution. This behavior is consistent with the presence of a finely dispersed metallic phase that can act as a physical barrier to grain boundary migration, thereby restricting alumina grain growth during sintering.

The relatively low standard deviation of ±0.21 μm confirms the high degree of microstructural uniformity within the ceramic matrix. This homogeneity is attributed to the slow heating rate up to 600°C, which enables uniform binder burnout and pore evolution. It is also due to the reducing Ar/H_2 atmosphere, which prevents oxidation of the nickel phase and limits undesirable interfacial reactions. Consequently, the mobility of Al_2O_3 grain boundaries is moderated, enabling densification without significant grain coarsening. The histogram shows that the applied sintering process creates a fine-grained alumina matrix with a controlled grain size distribution. This is beneficial because it maintains high hardness and strength while providing a stable ceramic framework for the embedded nickel phase. Preserving submicrometric Al_2O_3 grains is expected to positively impact the mechanical performance of the Al_2O_3-Ni composite by enhancing resistance to crack initiation and facilitating effective load transfer across ceramic-metal interfaces.

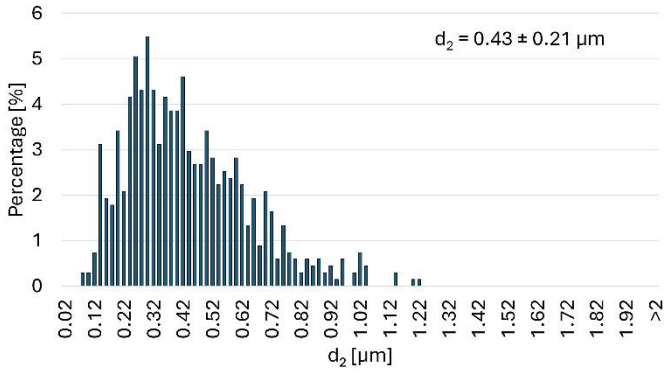

Figure 3. The histogram of the equivalent grain diameter (d2) of the Al2O3 grains in the Al2O3-Ni composite after sintering in a reducing Ar/H_2 atmosphere.

Figure 4 shows the results of an energy-dispersive X-ray spectroscopy (EDS) line scan conducted across the cross-section of the Al_2O_3-Ni composite that was fabricated using the centrifugal gel casting method. The line scan was acquired in the radial direction, spanning from the outer region, which is enriched in the metallic phase, to the inner, ceramic-dominated region, as shown in the corresponding backscatter electron (BSE) image. The EDS profiles clearly demonstrate a pronounced compositional gradient resulting from centrifugal processing. The Ni Kα signal intensity is highest at the beginning of the scan, corresponding to the outer zone of the sample, and decreases progressively with increasing distance along the scan line. Beyond the midpoint of the profile, the Ni signal drops to near-background levels, indicating strong depletion of the metallic phase in the inner region of the composite. This behavior is consistent with the significantly higher density of nickel compared to alumina, which promotes the outward migration of Ni particles under centrifugal acceleration during casting.

In contrast, the Al Kα and O Kα signals exhibit an opposite trend. In the outer, metal-rich region, the intensities of both aluminum and oxygen remain comparatively low, exhibiting noticeable local fluctuations. This reflects the heterogeneous distribution of alumina in the presence of a high volume fraction of nickel particles. As the scan progresses toward the inner

region, the Al and O intensities increase and stabilize, indicating the formation of a continuous, uniform Al_2O_3 matrix. The parallel evolution of the Al and O signals confirms the stoichiometric integrity of the alumina phase across the sample cross-section. The transition between the metal-rich outer zone and the ceramic-dominated inner zone is gradual, as evidenced by overlapping changes in Ni, Al, and O intensities over a finite distance. This smooth compositional transition corroborates the presence of a functionally graded microstructure, which is consistent with SEM observations and quantitative image analysis of the metallic phase distribution. The absence of sharp compositional discontinuities suggests stable slurry behavior and effective control of gelation kinetics during centrifugal forming. EDS line-scan analysis provides direct chemical evidence of the successful formation of a radially graded Al_2O_3-Ni composite characterized by a high nickel concentration in the outer region and progressively increasing alumina content toward the inner region.

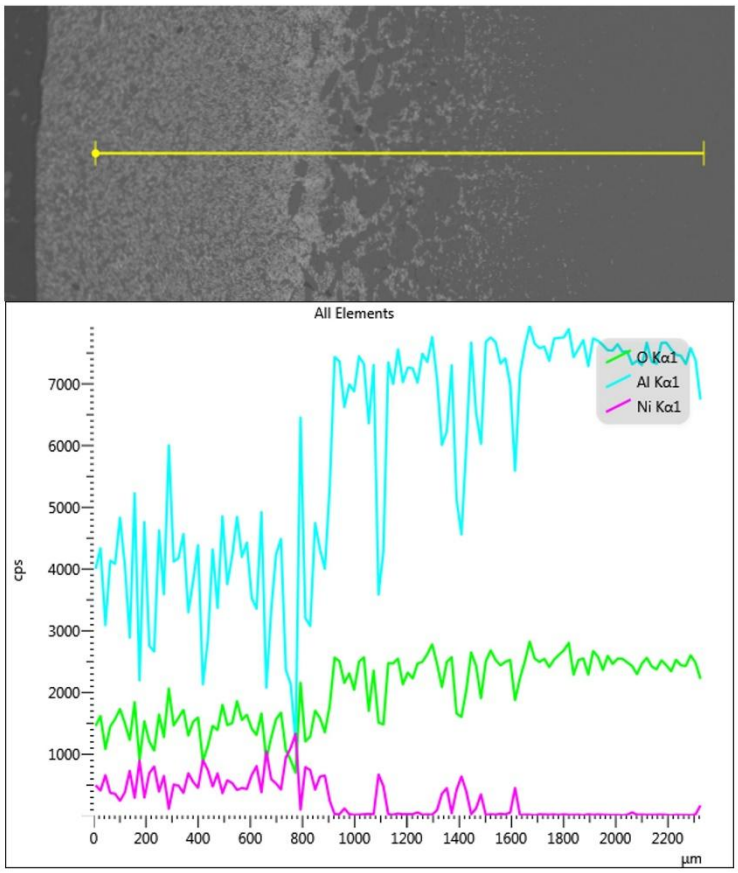

Figure 4. Backscattered electron (BSE) micrograph of the Al_2O_3-Ni composite fabricated by centrifugal gel casting with the corresponding EDS line-scan analysis performed along the radial direction of the sample.

Figure 5 shows the results of selected energy-dispersive X-ray spectroscopy (EDS) point analyses performed in the area near Zone II of the Al_2O_3-Ni composite that was made using centrifugal gel casting. This area corresponds to the transition region between the metal-enriched outer zone and the ceramic-dominated inner zone. Pronounced microstructural heterogeneity was observed in BSE-SEM imaging in this region. EDS spectra collected from points within the ceramic matrix (spectra 738 and 739) are dominated by strong Al Kα and O Kα peaks, confirming the presence of stoichiometric alumina. Quantitative analysis reveals aluminum and oxygen content of approximately 53–54 wt.% Al and 44–46 wt.% O, respectively, with only minor contributions from nickel (~1–2 wt.% Ni). The low Ni content detected in these locations is attributed to the proximity

of fine metallic particles or to the interaction volume of the electron beam rather than to solid solution formation or interfacial reaction products.

In contrast, spectra acquired directly from the bright contrast regions in the BSE image (spectra 736 and 737) exhibit intense Ni Kα and Ni Lα peaks. The quantitative results indicate approximately 100 wt.% Ni within the detection limits of the technique. The absence of detectable Al or O signals at these points confirms that the metallic phase remains chemically distinct and does not oxidize or interdiffuse with the alumina matrix during sintering in an Ar/H_2 atmosphere. The spatial correlation between the analysed points and the microstructural features visible in the SEM image shows a sharp compositional contrast between the alumina matrix and the nickel particles, even in the transition region. Importantly, no additional peaks associated with secondary phases or reaction products (e.g., $NiAl_2O_4$ spinel) were detected, indicating good chemical compatibility between Al_2O_3 and Ni under the selected processing and sintering conditions. EDS point analysis confirms that the Al_2O_3-Ni composite retains a two-phase microstructure consisting of chemically pure alumina and metallic nickel in the vicinity of Zone II, with phase separation preserved at the microscale. These results support the microstructural observations and validate the effectiveness of centrifugal gel casting combined with reducing-atmosphere sintering in producing stable, functionally graded ceramic-metal composites.

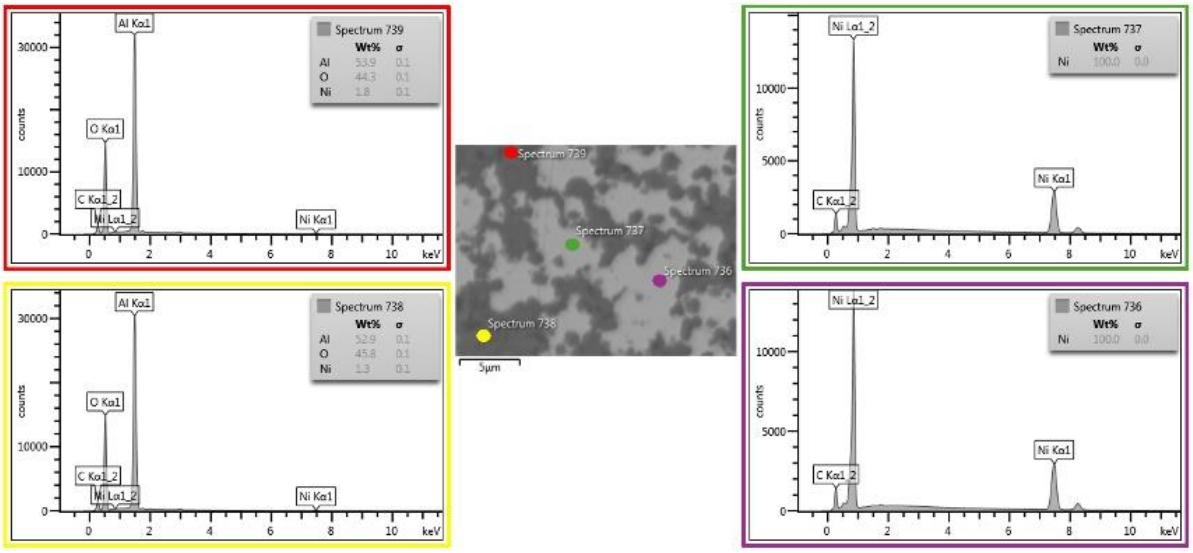

Figure 5. BSE–SEM image and corresponding EDS point analyses obtained from the region adjacent to Zone II of the Al_2O_3-Ni composite fabricated by centrifugal gel casting.

4. CONCLUSIONS

This work investigates the fabrication, densification behavior, and microstructural evolution of functionally graded Al_2O_3-Ni composites produced by centrifugal gel casting followed by sintering at 1400°C in a reducing Ar/H_2 atmosphere. Physical properties determined by the Archimedes method demonstrate near-theoretical densification, with a relative density of approximately 99%, low open porosity (~3.5%), and minimal water absorption (<1%), confirming the effectiveness of the processing route for producing compact ceramic–metal composites. Dimensional analysis reveals predictable and nearly isotropic shrinkage behavior during sintering, with linear shrinkage values of approximately 13–14% and a volumetric shrinkage of ~35%. Despite the presence of a radially graded microstructure induced by centrifugal forces, shrinkage anisotropy remains limited, indicating good control over slurry formulation, gelation kinetics, and thermal treatment. Detailed BSE-SEM observations, supported by quantitative image analysis and EDS measurements, show the formation of a well-defined three-zone radial architecture. The outer

zone is enriched with a high volume fraction of finely dispersed nickel particles forming a quasi-continuous metallic network.

In contrast, the inner zone is ceramic-dominated with only sparse, fine nickel dispersions. A transitional intermediate zone exhibits heterogeneous nickel clustering and a broader particle size distribution, reflecting the dynamic interplay between centrifugal segregation and increasing slurry viscosity during the gelation process. Research has shown that grain size analysis of the alumina matrix after sintering reveals a fine-grained, submicrometric microstructure with a narrow, unimodal size distribution. The controlled sintering schedule and reducing atmosphere effectively suppress abnormal grain growth and prevent interfacial reactions between Ni and Al_2O_3. EDS line scans and point analyses confirm a smooth compositional gradient across the composite cross-section and the chemical stability of both phases, with no evidence of secondary reaction products such as $NiAl_2O_4$ spinel. It should be emphasized that the study demonstrates the reproducible fabrication of dense, chemically stable, and functionally graded Al2O3-Ni composites through centrifugal gel casting, with controlled phase distribution and microstructural refinement.

This work makes several substantive contributions to the field of ceramic-metal composites and functionally graded materials. The study provides quantitative evidence that centrifugal gel casting can produce near-fully dense Al_2O_3-Ni composites with low open porosity and minimal water absorption, even in the presence of a strong compositional gradient. This validates the method as a reliable alternative to more complex or costly FGM fabrication techniques. The identification and systematic characterization of three distinct microstructural zones, metal-rich, transition, and ceramic-rich, offer new insight into phase segregation mechanisms during centrifugal gel casting. The work clarifies how density-driven particle migration and gelation kinetics jointly govern the spatial distribution of phases. By combining SEM image analysis, particle size histograms, and local volume fraction measurements, the study quantitatively demonstrates enrichment of fine nickel particles in the outer region and near-complete depletion in the inner region. This level of quantitative microstructural mapping strengthens understanding of centrifugal segregation phenomena. Based on the obtained results, it was found that EDS line scans and point analyses confirm that nickel remains metallic and chemically distinct from the alumina matrix after sintering, with no detectable interfacial reaction products. This contributes valuable experimental confirmation of phase compatibility under controlled reducing atmospheres.

What's more, one might be tempted to say that the work shows that pronounced compositional gradients can be introduced without inducing excessive shrinkage anisotropy or sintering defects. This is particularly relevant for near-net-shape manufacturing of graded components with tight dimensional tolerances. Moreover, based on the experiments carried out, it can be concluded that the preservation of a fine, submicrometric alumina grain size, despite the presence of a metallic phase, highlights the role of processing and sintering control in maintaining mechanical integrity. This finding is crucial for designing FGMs that strike a balance between toughness enhancement and high stiffness and hardness. Collectively, these contributions advance both the processing science and microstructural understanding of functionally graded ceramic-metal composites, with clear implications for structural and functional applications requiring spatially tailored properties.

Author Contributions: Conceptualization: Justyna Zygmuntowicz; Methodology: Justyna Zygmuntowicz; Software: Justyna Zygmuntowicz, Joanna Tańska, Paulina Wiecińska, Paulina Piotrkiewicz, Katarzyna Konopka, Mikołaj Szafrana, Marcin Wachowski, Joanna Szymańska, Waldemar Kaszuwara; Validation: Justyna Zygmuntowicz; Formal analysis: Justyna Zygmuntowicz; Writing – original draft preparation: Justyna Zygmuntowicz; Writing – review and editing: Justyna Zygmuntowicz; Supervision: Justyna Zygmuntowicz.

Funding: This publication was supported by grant No. TANGO-V-A/0004/2021 from the National Centre for Research and Development.

Conflicts of Interest: The authors declare no conflict of interest.

Data Availability Statement: Data available on request: «The data that support the findings of this study are available from the corresponding author upon reasonable request».

Declaration of Generative AI and AI-assisted technologies in the writing process: The authors declare that no generative AI or AI-assisted technologies were used in the writing of this manuscript.

REFERENCES

[1] Bassiouny Saleh, Jiang J., Fathi R., Al-Hababi T., Xu Q., Wang L., Song D., Ma A. (2020). 30 years of functionally graded materials: An overview of manufacturing methods, applications and future challenges. Composites Part B: Engineering, 201, 108376. https://doi.org/10.1016/j.compositesb.2020.108376.

[2] Veres C., Tănase M. (2025). A bibliometric review of 3D-printed functionally graded materials, focusing on mechanical properties. Machines, 13(3), 232. https://doi.org/10.3390/machines13030232.

[3] Li Y., Feng Z., Hao L., Huang L., Xin C., Wang Y., Bilotti E., Essa K., Zhang H., Li Z., Yan F., Peijs T. (2020). A review on functionally graded materials and structures via additive manufacturing: From multi-scale design to versatile functional properties. Advanced Materials Technologies, 5, 1900981. https://doi.org/10.1002/admt. 201900981.

[4] Wang C., Zhao S., Zhang Y., Zhang Y., Dong B., Yang J. (2025). Thermal and residual stress distributions of additively manufactured functionally graded materials. Mechanics of Advanced Materials and Structures, pp. 1–16. https://doi.org/10.1080/15376494.2025.2565007.

[5] Cao X.Q., Vassen R., Stoever D. (2004). Ceramic materials for thermal barrier coatings. Journal of the European Ceramic Society, 24 (1), pp. 1–10. https://doi.org/10.1016/S0955-2219(03)00129-8.

[6] Dejene B.K., Abtew M.A., Worku B.G. (2025). Smart core-sheath fibers for advanced textiles: Material integration, manufacturing strategies, and applications. Materials Today Advances, 28, 100655. https://doi.org/ 10.1016/j.mtadv.2025.100655.

[7] Ebrahimi M., Luo B., Wang Q., Attarilar S. (2024). High-performance nanoscale metallic multilayer composites: Techniques, mechanical properties and applications. Materials, 17(9), 2124. https://doi.org/ 10.3390/ma17092124.

[8] Clare A.T., Woizeschke P., Rankouhi B., Pfefferkorn F.E., Bartels D., Schmidt M., Wits W.W. (2025). Metal multi-material additive manufacturing: Overcoming barriers to implementation. CIRP Annals, 74(2), pp. 869–893. https://doi.org/10.1016/j.cirp.2025.05.004.

[9] Sharma S.K., Gajević S., Sharma L.K., Mohan D.G., Sharma Y., Radojković M., Stojanović B. (2025). Significance of the powder metallurgy approach and its processing parameters on the mechanical behavior of magnesium-based materials. Nanomaterials, 15(2), 92. https://doi.org/10.3390/nano15020092.

[10] Babalola B.J., Ayodele O.O., Olubambi P.A. (2023). Sintering of nanocrystalline materials: Sintering parameters. Heliyon, 9(3), e14070. https://doi.org/10.1016/j.heliyon.2023.e14070.

[11] Kumar N., Bharti A., Dixit M., et al. (2020). Effect of powder metallurgy process and its parameters on the mechanical and electrical properties of copper-based materials: Literature review. Powder Metallurgy and Metal Ceramics, 59, pp. 401–410. https://doi.org/10.1007/s11106-020-00174-1.

[12] Sonker P.K., Singh T.J., Srivastava A., Nahak B., Singh S.K. (2025). Advanced Engineering Materials, e2501452. https://doi.org/10.1002/adem.202501452.

[13] Jain R., Rangilal B., Bharat N., Bose P.S.C. (2023). Fabrication of ceramic composites from colloidal processing techniques for aerospace applications: A review. NanoWorld Journal, 9(S1), pp. S556–S561.

[14] Meshalkin V.P., Belyakov A.V. (2020). Methods used for the compaction and molding of ceramic matrix composites reinforced with carbon nanotubes. Processes, 8(8), 1004. https://doi.org/10.3390/pr8081004.

[15] Shvydyuk K.O., Lanceros-Mendez S., Silva A.P. (2025). Advanced ceramics in aerospace and defense: The interrelationship between traditional and additive manufacturing approaches. Advanced Materials Technologies, e01012. https://doi.org/10.1002/admt.202501012.

[16] Anil A., Nadimpalli R. (2026). Flexi mold slip casting: A novel integration of 3D printing with traditional manufacturing methods. Ceramics International, 52(1), pp. 974–988. https://doi.org/10.1016/j.ceramint. 2025.11.397.

[17] Tiller F.M., Tsai C.-D. (1986). Theory of filtration of ceramics: I. Slip casting. Journal of the American Ceramic Society, 69, pp. 882–887. https://doi.org/10.1111/j.1151-2916.1986.tb07388.x.

[18] Zuo K.H., Jiang D.L., Lin Q.L. (2006). Fabrication and interfacial structure of Al2O3/Ni laminar ceramics. Ceramics International, 32(6), pp. 613–616. https://doi.org/10.1016/j.ceramint.2005.04.027.

[19] Boch P., Chartier T., Huttepain M. (1986). Tape casting of Al2O3/ZrO2 laminated composites. Journal of the American Ceramic Society, 69, pp. C-191–C-192. https://doi.org/10.1111/j.1151-2916.1986.tb04836.x.

[20] Kedzierska-Sar A., Starzonek S., Kukielski M., Falkowski P., Rzoska S.J., Szafran M. (2019). Gelcasting of Al2O3-W composites: Broadband dielectric spectroscopy and rheological studies of tungsten influence on polymerisation kinetics. Ceramics International, 45(12), pp. 15237–15243. https://doi.org/10.1016/j.ceramint.2019.05.012.

[21] Haji M., Ebadzadeh T., Amin M.H., Kazemzad M., Talebi T. (2012). Gelcasting of Al2O3//Ag nanocomposite using water-soluble solid-salt precursor. Ceramics International, 38(1), pp. 867–870. https://doi.org/ 10.1016/j.ceramint.2011.06.062.

[22] Zygmuntowicz J., Tańska J., Wiecińska P., Piotrkiewicz P., Konopka K., Szafran M., Wachowski M., Michalski B., Kaszuwara W. (2025). Gradient Al2O3-Ni composites for aggressive substance transport: A novel approach using centrifugal gel casting. Composites Theory and Practice, 2, pp. 144–156. https://doi.org/10.62753/ctp.2025.09.2.2.

[23] Patel M. (2025). A comprehensive review of functionally graded materials and their ballistic impact performance: Current status and future challenges. Next Materials, 8, 100704. https://doi.org/10.1016/j.nxmate.2025.100704

[24] Ailawalia P., Gupta D. (2023). Two-dimensional deformations in a functionally graded orthotropic micropolar solid. Mechanics Based Design of Structures and Machines, 51(1), pp. 555–565. https://doi.org/ 10.1080/15397734.2020.1848589.

[25] Paulino G.H., Jin Z.-H., Dodds R.H., Sahu S.K., Badgayan N.D., Rama Sreekanth P.S. (2017). Failure of functionally graded materials. Reference Module in Materials Science and Materials Engineering, Elsevier. https://doi.org/10.1016/B978-0-12-803581-8.00875-4.

[26] Silva R.F., Coelho P.G., Gustavo C.V., Almeida C.J., Farias F.W.C.F., Duarte V.R., Xavier J., Esteves M.B., Conde F.M., Cunha F.G., et al. (2024). Functionally graded materials and structures: Unified approach by optimal design, metal additive manufacturing, and image-based characterization. Materials, 17(18), 4545. https://doi.org/10.3390/ma17184545.

[27] Zygmuntowicz J., Miazga A., Konopka K., Kaszuwara W. (2016). Structural and mechanical properties of graded composite Al_2O_3 /Ni obtained from slurry of different solid content. Procedia Structural Integrity, 1, pp. 305–312. https://doi.org/10.1016/j.prostr.2016.02.041.

[28] Żurowski R., Zygmuntowicz J., Tomaszewska J., Ulkowska U., Piotrkiewicz P., Wachowski M., Szachogłuchowicz I., Kukielski M. (2022). Sustainable ZTA composites produced by an advanced centrifugal slip casting method. Ceramics International, 48(8), pp. 11678–11695. https://doi.org/10.1016/ j.ceramint.2022.01.026.

[29] Kumar S.N.N. (2025). Development of controller-based interchangeable axis centrifugal casting machine and characterization of aluminum–silicon carbide (Al–SiC) functionally graded composite. Cureus Journal of Engineering. https://doi.org/10.7759/s44388-025-08227-0.

[30] Yawar J. (2025). A review of static and dynamic analysis in functionally graded materials with material nonlinearities. Mechanics of Solids, 60(4), 3031. https://doi.org/10.1134/S0025654425601764.

[31] Karimzadeh M., Basvoju D., Vakanski A., Charit I., Xu F., Zhang X. (2024). Machine learning for additive manufacturing of functionally graded materials. Materials, 17(15), 3673. https://doi.org/10.3390/ ma17153673.